Single-photon detection using a quantum dot optically gated field-effect transistor with high internal quantum efficiency

M. A. Rowe,[a] E. J. Gansen, M. Greene, R. H. Hadfield, T. E. Harvey, M. Y. Su, S. W. Nam, and R. P. Mirin
Optoelectronics Division, National Institute of Standards and Technology, Boulder, Colorado 80305

D. Rosenberg
Los Alamos National Laboratory, Los Alamos, New Mexico 87545

(Received 14 August 2006; accepted 27 October 2006; published online 19 December 2006)

We investigate the operation of a quantum dot, optically gated, field-effect transistor as a photon detector. The detector exhibits time-gated, single-shot, single-photon sensitivity, a linear response, and an internal quantum efficiency of up to (68±18)% at 4 K. Given the noise of the detector system, they find that a particular discriminator level can be chosen so the device operates with an internal quantum efficiency of (53±11)% and dark counts of 0.003 counts per shot. © *2006 American Institute of Physics*. [DOI: 10.1063/1.2403907]

Single-photon detectors are crucial components in the areas of quantum optics and quantum cryptography and at the frontiers of low-light imaging in medicine, astronomy, and chemistry. Recently, detectors have been demonstrated that utilize the photoconductive gain[1] associated with storing photo-generated charge carriers in the vicinity of a two-dimensional electron gas (2DEG) in specially designed field-effect transistors (FETs). Approaches to the charge storage in these detectors have included electrostatic confinement using metallic gates,[2,3] naturally occurring defect centers in AlGaAs,[4] and self-assembled quantum dots (QDs).[5,6] One of the keys to making such a detector efficient is to trap a high percentage of the carriers (either electrons or holes) excited in the device. Here, we investigate the operation of a semiconductor quantum dot optically gated field-effect transistor (QDOGFET) that is specially designed to efficiently trap photogenerated holes in a layer of self-assembled QDs. In this device, high internal quantum efficiency (IQE) is achieved by using an electric field to direct the holes generated in the absorbing region of the detector to the QDs where ~70% are trapped. We show that the detector exhibits single-photon sensitivity, a linear response to the average number of photons, and can operate with relatively low dark counts.

Figure 1 shows the composition and band structure of the QDOGFET. The device was fabricated from a semiconductor heterostructure grown by molecular beam epitaxy on a GaAs substrate. The heterostructure consists of a 200 nm GaAs buffer layer, a 230 nm $Al_{0.20}Ga_{0.80}As$ layer, a Si δ-doped ($\sim 1\times10^{12}$ cm^{-2}) layer, a 70 nm $Al_{0.20}Ga_{0.80}As$ layer, a 100 nm GaAs absorbing layer, an InGaAs QD layer, a 200 nm $Al_{0.20}Ga_{0.80}As$ layer, and a 10 nm n-doped ($\sim 6\times10^{17}$ cm^{-3}) GaAs cap layer. The δ-doping provides excess electrons to the conduction band forming a 2DEG at the interface of the GaAs absorbing layer and the AlGaAs layer (shown in Fig. 1) as well as to a secondary 2DEG at the interface of the AlGaAs layer and the GaAs buffer layer. The device was fabricated by etching a channel mesa (3.9 μm wide and 17 μm long) between Au/Ni/Ge source and drain Ohmic contacts and by depositing a 0.68 μm long, 4 nm thick, semitransparent Pt Schottky barrier gate midchannel. The photosensitive, or active, area of the device is the gated channel region, which is 2.7 μm^2 and contains ~1000 QDs. Although some parallel conduction from the secondary 2DEG was detected through the source and drain contacts, the dependence of the conductance of the two 2DEGs on the gate bias was very different. This allowed us to operate the device at a reverse gate bias such that the transconductance was dominated by the primary 2DEG shown in Fig. 1. In addition to the QDOGFET described above, two control devices were also fabricated to investigate secondary sources of photogenerated signals. One of the devices was fabricated with an opaque gold gate to quantify signals produced from photons absorbed outside the active area, and the other device was fabricated from a twin wafer grown without QDs.

Our QDOGFET is designed (see Fig. 1) to efficiently detect photons absorbed in the GaAs absorbing layer. An incident photon with the appropriate energy creates an electron-hole pair in the GaAs absorbing layer. With a reverse bias applied to the gate, the electric field directs the electron to the 2DEG shown in Fig. 1 and the hole to the QDs, where it is trapped. This positively charged hole screens the bias field, effectively changing the gate bias by a positive amount, and increases the channel current, I_{ds}. It can be shown[7] that, given a constant potential between the gate and 2DEG, the change in I_{ds} caused by the addition of N_{QD} positive charges to the QD plane is

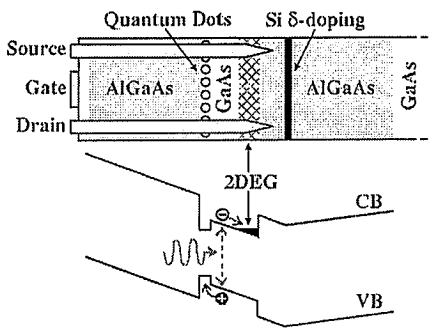


FIG. 1. Schematic diagrams of the composition and band structure of the QDOGFET. CB and VB denote the conduction and valence bands, respectively.

[a]Electronic mail: mrowe@boulder.nist.gov

 © 2006 American Institute of Physics
Downloaded 14 Feb 2007 to 132.163.53.60. Redistribution subject to AIP license or copyright, see http://apl.aip.org/apl/copyright.jsp

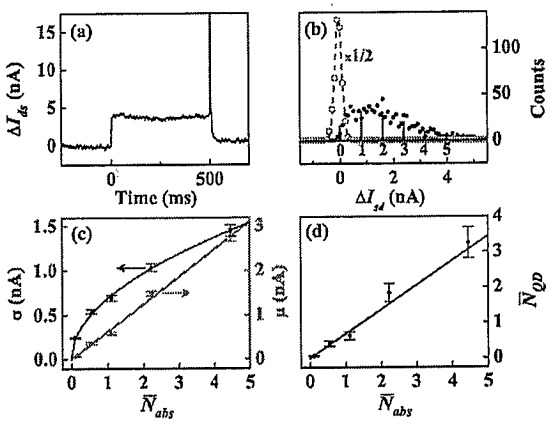


FIG. 2. (a) Typical temporal response (change in the drain-source current, ΔI_{ds}) of the QDOGFET for $\bar{N}_{abs}$=2.2. (b) Step height distributions with (solid circles) and without (open circles) laser illumination. The dashed curve is a Gaussian fit to the nonilluminated data, and the solid curve is the ideal Poisson distribution for 1.8 mean photoevents (numbers below curve label the individual events). (c) Statistics (mean μ and standard deviation σ) of the step height distributions acquired as a function of $\bar{N}_{abs}$. (d) $\bar{N}_{QD}$ calculated from μ and σ as a function of $\bar{N}_{abs}$. In (c) and (d), the solid curves represent functional fits to the data.

$$\Delta I_{ds} = g_m \frac{eW}{\varepsilon' A} N_{QD}. \quad (1)$$

Here g_m is the FET transconductance, e is the elementary charge, W is the distance between the gate and the QD layer, ε' is the electric permittivity of $Al_{0.20}Ga_{0.80}As$, and A is the active area of the device. Over time, the charging of the QDs caused by even a single carrier results in a large change in the cumulative charge transferred in the channel (a small change in the channel current integrated over a long period). This photoconductive gain makes the device very sensitive to illumination with light of the appropriate photon energy.

We examined the ability of the QDOGFET to detect single photons by illuminating the device with highly attenuated laser pulses (0.5 Hz repetition rate) and by monitoring the change in I_{ds}. During these measurements the QDOGFET was cooled to 4 K in a liquid helium cryostat, and the spot size (40 μm $1/e$ diameter) of the incident pulses was kept large enough to provide uniform illumination of the active area. The photon energy (1.54 eV) of the pulses was tuned above the band gap of GaAs but below the band gap of AlGaAs to ensure that electron-hole pairs were generated in the GaAs absorbing layer. Each laser pulse was followed by an electrical reset 500 ms later, where the gate-source bias was raised to +1 V for 1 ms. This resulted in a flow of electrons into the QDs, where they recombined with the trapped holes, leaving the QDs empty.

Typical results of these measurements are shown in Figs. 2(a) and 2(b), where the device was illuminated with a train of 20 μs laser pulses. The mean number of photons absorbed in the GaAs absorbing region per pulse, $\bar{N}_{abs}$, was 2.2. Figure 2(a) shows the temporal response of the detector to one of the laser pulses. At t=0 we observe a well-defined step in I_{ds} that coincides with the arrival of the laser pulse and shows little decay over the 500 ms shown. When the device is reset I_{ds} spikes and quickly returns to its preillumination value. The persistent photoconductivity and electrical reset are consistent with prolonged trapping of the photoexcited holes in the QDs, as has been reported in previous works.[8,9] Figure 2(b) shows the distribution of step heights measured for a train of laser pulses along with the distribution obtained without illumination. Here the step height is determined for each shot by averaging the measured current over 50 ms windows leading up to and following a 10 ms temporal gate surrounding the arrival of each laser pulse and then subtracting the two averaged values. The histogram without illumination is well fitted by a Gaussian function with a full width at the $1/e$ points of 0.4 nA. By contrast, the histogram obtained with illumination is asymmetrically distributed about its nonzero mean, characteristic of Poisson statistics of a small number of photons.

From the distribution statistics, we determine the efficiency of the detection process by evaluating the mean number of holes that are trapped in the QDs per laser pulse, $\bar{N}_{QD}$. For Poisson statistics, $\bar{N}_{QD}=(\mu/\sigma)^2$, where μ is the mean step height and σ is the standard deviation of the distribution. In order to get an accurate value for $\bar{N}_{QD}$, it is important to eliminate contributions to μ and σ not associated with the QDs under the gate. To do this, we perform identical measurements using (1) a control FET without QDs to verify that the current changes observed for the QDOGFET were associated with QDs and (2) a QDOGFET fabricated with an opaque gold gate to quantify any signals from the ungated portions of the channel. For the device without QDs, we observed only very small laser-induced steps in I_{ds} when operating the device at similar gate biases as used in acquiring the data shown in Fig. 2. These steps were on average ~10% of the height of the current changes observed in Fig. 2 and did not reset as effectively as those signals, verifying the role of the QDs as the dominant storage mechanism for the QDOGFET. We believe that the small non-QD related signals are caused by the capture of charge carriers in dilute traps[4] in the thick GaAs buffer layer, which absorbs any photons transmitted by the absorbing layer. These trapped carriers affect the conductance of the secondary 2DEG discussed previously; however, since the transconductance associated with this conduction path is very small, the contributions of these non-QD related signals are much smaller than those caused by charged QDs. We observed much larger laser-induced steps in I_{ds} of the device without QDs by operating the FET at much different gate biases where the transconductance associated with the secondary 2DEG is comparable to that of the primary 2DEG shown in Fig. 1. When the device fabricated with an opaque gold gate was used, we observed laser-induced steps in I_{ds} that were on average ~20% of the height of the steps plotted in Fig. 2. These signals appeared only when the channel regions very close to the gate edges were illuminated, indicating that these signals are associated with fringe fields that extend past the edges of the physical gate.

Taking both of the parasitic effects discussed above into account, a calculation of $(\mu/\sigma)^2$ for the data shown in Fig. 2(b) yields $\bar{N}_{QD}$=1.8. From this value, we find that each trapped hole changes I_{ds} by 0.8 nA, on average. This value compares quite well with the expected current change calculated from Eq. (1), where for our experimental parameters ΔI_{ds} caused by a single trapped hole is calculated to be 0.7 nA. The subphoton sensitivity of the detector is illustrated graphically in Fig. 2(b), where the ideal Poisson distribution for 1.8 mean photoevents is superimposed on the

Downloaded 14 Feb 2007 to 132.163.53.60. Redistribution subject to AIP license or copyright, see http://apl.aip.org/apl/copyright.jsp

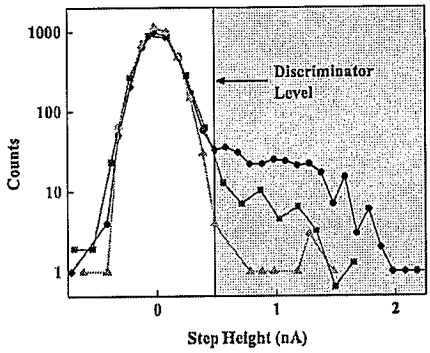


FIG. 3. Step height distributions acquired using the primary QDOGFET without laser illumination (triangles) and for $\bar{N}_{abs}$=0.11 (circles). Squares are data obtained using the device with an opaque gold gate for the same illumination conditions as for the circles.

data. Notice that the experimental data follow the envelope of the ideal distribution, where the position of the single-photon peak is well separated from the distribution acquired in the absence of illumination. The fact that the individual photoevents are not resolvable is probably due to nonuniformities in the step heights caused by the parasitic effects discussed in the previous paragraph (i.e., the edge effects and the capture of charge carriers in dilute traps in the GaAs buffer layer) coupled with detector noise.

In Fig. 2(c), the step height distribution statistics (μ and σ) are plotted as a function of $\bar{N}_{abs}$. The vertical error bars are based on the measurement statistics. As expected for Poisson statistics, μ and σ exhibit linear and square-root dependences on $\bar{N}_{abs}$, respectively. The resulting linear dependence of $\bar{N}_{QD}$ on $\bar{N}_{abs}$ is illustrated in Fig. 2(d). A weighted fit of the data yields a slope of (68±18)%, representing the IQE of the detector. The error stated incorporates scatter in the data as well as uncertainties in laser power, attenuation, experimental geometry, and absorption.

In the above analysis of the efficiency of the QDOGFET, every photoinduced change in I_{ds} occurring within the temporal gate was taken into account; however, in practice, only signal changes above some discriminator level should be counted in order to reduce the probability of mistaking a dark count caused by noise for a real photon count. We investigated the trade-off between the quantum efficiency and the dark counts for the QDOGFET detector by illuminating the device with very low-photon-flux pulses, where the probability of absorbing more than one photon in the active area for a given laser pulse was very small. In this case, the correspondence between photocounts and trapped holes is nearly one-to-one. Results of these measurements are shown in Fig. 3, where the distributions of step heights obtained with our primary QDOGFET are plotted for $\bar{N}_{abs}$=0.11 and in the absence of illumination. Also plotted in the figure is the distribution of step heights obtained when illuminating the companion device with an opaque gold gate with pulses of the same incident photon flux as used in illuminating the primary QDOGFET. The histogram obtained for the primary QDOGFET under illumination is composed of two main parts: a sharp Gaussian feature centered at the origin, representing current changes resulting from random noise, and a pronounced shoulder. The drastic reduction of the shoulder in the absence of the illumination indicates that it is dominated by photoinduced counts with very few dark counts. In addition, the suppression of this shoulder for the device with the opaque gold gate indicates that it is largely dominated by counts caused by single photons absorbed in the active region of the device. By summing these photocounts (and eliminating the counts attributed to edge effects) registered above a chosen threshold current, we evaluate the efficiency of the device for that particular discriminator level. For example, for a discriminator level of 0.48 nA we find that the IQE of the detector is (53±11)% with corresponding dark counts of 0.003 counts per shot.

In conclusion, we have investigated the operation of a QDOGFET detector that exhibits time-gated, single-shot, single-photon sensitivity, a linear response to average photon number, and an IQE of ~70%. Our measurements indicate that by choosing an appropriate discriminator level, the detector can operate with relatively low dark counts without significantly degrading the efficiency of the detector. While the internal efficiency of the device is quite high, we note that the overall detection efficiency (fraction of photons incident on the active area that are counted) is 2%–3% and is currently limited by the 38% transmission of the Pt gate and the 10% absorption of the active GaAs layer. It should be possible to construct devices that exhibit detection efficiencies that approach their internal efficiencies by optimizing the thickness of the absorbing layer and by positioning the layer inside a resonant cavity. These modifications would also reduce secondary signals caused by absorption of photons in the thick GaAs buffer layer. Also, by masking the edges of the active area with an opaque material we can limit the QDs available for charge storage to those in the interior of the gated region. These modifications are expected to improve the uniformity of the photoinduced steps in I_{ds}, potentially making the detector capable of high-efficiency photon number resolution, as predicted by Eq. [1]. Further studies will also focus on optimizing the size and aspect ratio of the active region of the detector (a large active area is desired for efficient optical coupling), constructing detectors suitable for communication wavelengths through modified material compositions, and operating the device at increased speeds. While here we report on our QDOGFET detector at a 0.5 Hz detection rate, a similar device has been shown[6] to operate at much higher frequencies, and it is reasonable to expect that our detector will operate at higher speeds as well.

Support for this project has been provided by the Disruptive Technology Office (DTO).

[1]A. Rose, *Concepts in Photoconductivity and Allied Problems* (Interscience, New York, 1963).
[2]H. Kosaka, D. S. Rao, H. D. Robinson, P. Bandaru, K. Makita, and E. Yablonovitch, Phys. Rev. B **67**, 045104 (2003).
[3]D. S. Rao, T. Szkopek, H. D. Robinson, and E. Yablonovitch, J. Appl. Phys. **98**, 114507 (2005).
[4]H. Kosaka, D. S. Rao, H. D. Robinson, P. Bandaru, T. Sakamoto, and E. Yablonovitch, Phys. Rev. B **65**, 201307(R) (2002).
[5]A. J. Shields, M. P. O'Sullivan, I. Farrer, D. A. Ritchie, R. A. Hogg, M. L. Leadbeater, C. E. Norman, and M. Pepper, Appl. Phys. Lett. **76**, 3673 (2000).
[6]B. E. Kardynal, A. J. Shields, N. S. Beattie, I. Farrer, K. Cooper, and D. A. Ritchie, Appl. Phys. Lett. **84**, 419 (2004).
[7]G. Yusa and H. Sakaki, Electron. Lett. **32**, 491 (1996).
[8]A. J. Shields, M. P. O'Sullivan, I. Farrer, D. A. Ritchie, K. Cooper, C. L. Foden, and M. Pepper, Appl. Phys. Lett. **74**, 735 (1999).
[9]D. Heinrich, J. Hoffmann, J. J. Finley, A. Zrenner, G. Bohm, and G. Abstreiter, Physica E (Amsterdam) **7**, 484 (2000).

Downloaded 14 Feb 2007 to 132.163.53.60. Redistribution subject to AIP license or copyright, see http://apl.aip.org/apl/copyright.jsp